Journal of Power Sources 269 (2014) 111–116

Contents lists available at ScienceDirect

Journal of Power Sources

journal homepage: www.elsevier.com/locate/jpowsour

Key parameters in design of lithium sulfur batteries

Ning Ding [a], Sheau Wei Chien [a], T.S. Andy Hor [a, b], Zhaolin Liu [a, *], Yun Zong [a, *]

[a] Institute of Materials Research and Engineering (IMRE), A*STAR (Agency for Science, Technology and Research), 3 Research Link, Singapore 117602, Republic of Singapore

[b] Department of Chemistry, National University of Singapore, 3 Science Drive 3, Singapore 117543, Republic of Singapore

HIGHLIGHTS

- Studied the effect of the carbon to sulfur ratio on the performance of Li–S batteries.
- Investigated the influence of sulfur loading density and electrolyte volume on cell capacity.
- Provided a guideline for the design of high performance Li–S batteries.

GRAPHICAL ABSTRACT

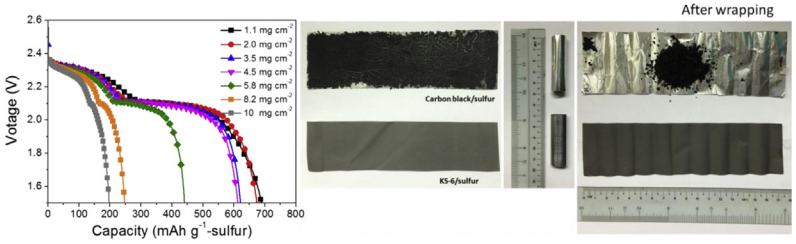

ARTICLE INFO

Article history:
Received 21 May 2014
Received in revised form
25 June 2014
Accepted 1 July 2014
Available online 9 July 2014

Keywords:
Lithium sulfur battery
Carbon to sulfur ratio
Sulfur loading density
Electrolyte volume
Deformability

ABSTRACT

In this paper, we discuss some key parameters in design of lithium sulfur batteries with high energy density, in particular carbon/sulfur ratio, sulfur loading density, electrolyte volume and electrode deformability, which directly impact the battery performance in terms of capacity, cycleability, and processibilities, etc. We find that a carbon to sulfur ratio of 1:2 (w/w) in the electrode is good for high specific capacity, giving a capacity of 538 mA h g^{-1} which is 3 times as high as that of $LiCoO_2$ cathode. The issue of fragileness for electrode at high sulfur loading density is mitigated by replacing carbon black with fine graphite powders. With these optimizations the carbon–sulfur electrode gives an energy density of 5.88 mW h cm^{-2} which corresponds to 60% of that of the commercial $LiCoO_2$ electrode.

1. Introduction

Lithium-ion (Li-ion) batteries have dominated the power supply market of portable electronic devices since the first launch of commercial lithium cobalt oxide/carbon ($LiCoO_2$/C) cells by Sony in 1991. Though being widely used the Li-ion batteries are seeing their bottlenecks in energy density limited by the lithium capability of lithium transition metal oxide (Li-M-O, M = Ni, Co and Mn) cathodes which typically deliver a theoretical specific capacity in the range of 120–320 mA h g^{-1} [1,2]. To meet the ever-growing demands on rechargeable batteries with higher energy density, non-lithium intercalated transition metal oxides, such as Me_xO_y (Me = V [3–5] or Cr [6]) and group 16 (VIA) elements (primarily oxygen [7], sulfur[8] and selenium [9]), have recently been exploited as the cathode materials for next-generation lithium batteries. For these non-lithium intercalated cathodes, lithium is used as the counter anode. In this case extra care in safety is required, as the growth of dendrites may cause short-circuit and explosion if the electrode is not properly engineered. Lithium–sulfur (Li–S) system is considered as the safest among batteries using lithium metal as anode, as its discharged products, lithium polysulfides, are soluble in the electrolyte that significantly suppress the formation of lithium dendrites [10]. Li–S battery is also a choice for its high energy

* Corresponding authors.
E-mail addresses: zl-liu@imre.a-star.edu.sg (Z. Liu), y-zong@imre.a-star.edu.sg (Y. Zong).

http://dx.doi.org/10.1016/j.jpowsour.2014.07.008
0378-7753/

density. Theoretically, sulfur can deliver a specific capacity of 1672 mA h per gram sulfur (mA h g^{-1}-sulfur) that is nearly 5 times as high as that of Li-ion batteries [11]. Furthermore, Li–S battery is a cost-effective choice, as sulfur is obtained from the byproducts of oil refining with the annual world production of 69 million tons (Mt) in 2011 [12] which is sufficient for 4 billions of 60 kW automobiles.

So far, major efforts in the Li–S battery research have been the development of sulfur composites with various microstructures for the cathode, and some interesting findings were reported [13–23]. For sulfur cathode, one has to deal with its poor intrinsic electrical conductivity (1×10^{-15} S m^{-1}) by incorporating large portion of carbon black, which lowers the sulfur content and reduces the gravimetric and volumetric energy density at cell level [24]. High sulfur content (up to 70 wt%) can be achieved by incorporating sulfur into highly ordered mesoporous carbon, followed by coating with polyethylene glycol [25], or using a lower load of graphene or carbon nanotubes as substitute of carbon black [26–30]. More recently, the concept of forming a yolk-shell structure with internal void space to tolerate the volume expansion of sulfur during discharge was proposed by Cui et al. [13,23,31] and the composites exhibited distinctly improved cycling performance (>1000 cycles). Though these new cathode materials shed a light on Li–S battery research, the actual progress was far insufficient for practical application. For example, in these studies the sulfur loading density was less than 1 mg cm^{-2} [32–38]. In this case the theoretical overall cathode capacity per unit area is about 60% of that of $LiCoO_2$ cathode in a commercial Li-ion batteries and the energy density is merely about 35% due to the lower working voltage of Li–S system. To compete with lithium-ion batteries using $LiCoO_2$ electrode, one would need a minimum sulfur loading density of 3 mg cm^{-2} in the cathode. Some high sulfur loading density cases have been reported [39–42]; however, a high sulfur loading density often associates with mechanical failure of the electrode film, e.g. cracking and/or peeling, leading to poor battery performance. It remains a challenge to develop high quality sulfur electrode for high performance Li–S batteries.

Apart from cathode materials, the selection of electrolyte is crucial for Li–S batteries [43]. The electrolyte is the media that transports lithium ions and dissolves polysulfides (PS) which significantly impacts the overall electrochemical performances of Li–S battery [44]. Electrolyte with low viscosity and high PS solubility generally favors the cell reaction; however, the dissolution of PS imposes negative impact on coulombic efficiency and capacity retention. Such negative impact can be suppressed by the introduction of $LiNO_3$ additive into the electrolyte [45]. During the discharge process, sulfur is gradually reduced to soluble PS (Li_2S_8, Li_2S_6 and Li_2S_4). Li_2S_4 is further reduced to insoluble sulfides (Li_2S_2 and Li_2S) that precipitate on the carbon surface at the end of discharge. In the reversed charge process, insoluble PS is first oxidized into soluble PS which is further converted into sulfur and eventually precipitates on the carbon surface when charge is completed. The excess amount of PS in the electrolyte may cover the sulfur surface as a nonconductive coating and adversely impact the following discharge performance. Moreover, the amount of electrolyte also affects the cell performance. Larger volume of electrolyte generally leads to a higher initial discharge capacity [46]; however, it reduces the energy density of the cell. Therefore, it is critical to balance the volume of electrolyte and the amount of sulfur for high performance Li–S batteries.

In this work, we prepared a series of carbon/sulfur (C/S) composites with a different weight ratio (3:1, 2:1, 1:1, 1:2 and 1:3) and evaluated their electrochemical performances in Li–S batteries. A high sulfur content and crack-free electrode with a loading density of 10 mg cm^{-2} was fabricated, as carbon black was substituted by fine graphite powders. The effect of the volume of electrolyte on the electrochemical performances was also investigated.

2. Experimental

C/S composites were prepared by manually mixing carbon black (Denka) or synthetic graphite (KS-6, TIMREX®) with precipitated sulfur (99.5%, Alfa Aesar) in different weight ratios in an agate mortar. The mixture of C/S composite (95 wt.%) and poly(vinylidene fluoride) (PVDF, Solef® 5130, 5 wt.%) was dispersed in 1-methyl-2-pyrrolidinone (NMP) to form a slurry which was subsequently casted onto Al foil as a current collector. After drying for 2 h in air at 80 °C, electrode discs of 15 mm in diameter were punched out (without pressing) and transferred into an argon-filled glovebox (MBraun) for assembly. The electrolyte used was 1 M lithium bis(tri-fluoromethanesulfonyl)imide (LiTFSI) in solvent mixture of 1,2-Dimethoxyethane (DME) and 1,3-Dioxolane (DOL) (v/v, 1:1) with 0.725 mol L^{-1} of lithium nitrate ($LiNO_3$) as additive. Li–S coin cells (CR2032) were assembled with Li metal as counter electrode. One pair of wave spring and spacer was used to make the cell full-filled. The cathode and Li anode were separated by an Asahi separator with a thickness of 16 μm. The cells were tested on a multi-channel battery tester (Shenzhen Neware Co. Ltd.) at a constant current of 0.1 mA. The cycling voltage range was between 1.5 and 3.2 V (all the voltage mentioned in this work is vs. Li^+/Li).

3. Results and discussion

3.1. Optimization of carbon–sulfur ratio

As sulfur exists in its allotrope of octasulfur (cyclo-S_8), the S_8 rings are opened during the discharge and some of the resultant S_8 chains are further cut shorter. Subsequently, these sulfur with different chain lengths are reduced to a series of Li_2S_n ($n = 4–8$) which are soluble in electrolyte, exhibiting a voltage slope at 2.3 V. Theoretically this step is anticipated to deliver a specific capacity of 418 mA h g^{-1}-sulfur; however, in practice the capacity is often affected by incomplete utilization of sulfur, especially if the sulfur particle size is too big. In the followed step, soluble Li_2S_n are further reduced to form insoluble Li_2S_2 and Li_2S as precipitate on carbon matrix, leading to a long voltage plateau at 2.1 V. This process delivers a theoretical specific capacity of 1254 mA h g^{-1}-sulfur. Assuming that sulfur was fully converted into Li_2S_n in the first step, the capacity at the second step should be mainly influenced by the property of the carbon matrix. Generally, larger surface area accommodates more Li_2S_2 and Li_2S precipitates, and higher conductivity allows for easier conversion of Li_2S_2 to Li_2S. It is noteworthy here that the cycling performance of Li–S batteries can be affected by the nucleation and growth of Li_2S_2/Li_2S [47]. As the cell was further discharged to 1.5 V, another slope at 1.7 V from the reduction of $LiNO_3$ appeared [48]. The electrolyte additive, $LiNO_3$, is used to stabilize Li anode by the formation of an enhanced solid electrolyte interface (SEI) film, which can improve the coulombic efficiency of Li–S batteries [49].

As sulfur has poor electronic conductivity, it needs to be blended or combined with a conductive agent, e.g. carbon black, to form C/S composites as working cathode. High sulfur content in the C/S composite favors high energy density; however, too low carbon content will lead to the formation of electrically isolated islands in the electrode. Consequently, the sulfur utilization rate will be low (affecting the capacity delivered at 2.3 V), and so does the subsequent precipitation of soluble Li_2S_n (causing capacity loss at the voltage plateau of 2.1 V). It is thus crucial to have a balanced carbon to sulfur ratio in the C/S composite cathode. As for the carbon sources, some recent work reported carbon black as a good

candidate for Li–S batteries [50]. The performance of batteries using electrode of C/S composites with different ratio of Denka black to sulfur is shown in Fig. 1a. As expected, at the C/S ratio of 1:3 (high sulfur content), the specific capacity was about 466 mA h g^{-1}-sulfur which is only about 27.9% of the theoretical value (1672 mA h g^{-1}-sulfur). Table 1 summarizes the capacities attributed to the tree cell reactions discussed above for C/S composites with different C/S ratio. It is clearly seen that for the composite with a C/S ratio of 1:3, 62.7% of sulfur was reduced to Li_2S_n (262 mA h g^{-1}-sulfur in experiment *vs* 418 mA h g^{-1}-sulfur in theory), and the conversion of Li_2S_n to Li_2S after fully discharged was as low as 13.9% (174 mA h g^{-1}-sulfur in experiment *vs* 1254 mA h g^{-1}-sulfur in theory). Such low conversion is likely due to the unavailability of sufficient carbon surface that can accommodate the precipitation of Li_2S_2 and Li_2S. This hypothesis is verified when the C/S ratio was increased from 1:3 to 1:2, where a 2 times of capacity increase is seen from the step of Li_2S_n reduction to Li_2S (538 mA h g^{-1}-sulfur *vs* 174 mA h g^{-1}-sulfur). As the C/S ratio was further increased to 1:1, the sulfur utilization rate at first reduction plateau increases to 78.5% (328 mA h g^{-1}-sulfur *vs* 418 mA h g^{-1}-sulfur) and more capacity was delivered by the reduction reaction of Li_2S_n (758 mA h g^{-1}-sulfur *vs* 538 mA h g^{-1}-sulfur). At the carbon content of 50 wt% and higher, the capacities from the reduction of cyclo-S_8 to soluble Li_2S_n and from the reduction of Li_2S_n to Li_2S started to decrease slowly. This may be due to the increased self-discharge reaction and the precipitation of Li_2S on Li anode. In general, self-discharge rate of Li–S batteries is higher than that of Li-ion batteries due to the existence of PS redox shuttle that reacts with Li to form precipitates on the anode. This phenomenon is even more pronounced for the samples with higher C/S ratios. Typically, loading of C/S composites in electrode was 1.7 mg cm^{-2} in this work. In this case, sulfur is insufficient to compensate the loss due to its precipitation onto the Li anode. In addition, a long voltage slope is observed at 1.7 V for the composite with high carbon content which is attributed to the reduction of $LiNO_3$ on carbon matrix ($LiNO_3 + 2Li^+ + 2e \rightarrow LiNO_2 + Li_2O$). Such reduction is irreversible in the voltage window of 1.5–3.2 V, leading to the formation of a stable passivation layer on the carbon matrix. This is confirmed by the disappearance of the voltage slope at 1.7 V in the following cycles. Fig. 1b presents the relationship between C/S ratio and specific capacity (per gram electrode, including sulfur, carbon and binder) in 2nd cycle. A maximum capacity of 538 mA h g^{-1}-electrode was achieved for the composite with C/S ratio of 1:2, which is 3 times higher than that of $LiCoO_2$ cathode (130 mA h g^{-1}-electrode, assuming with 5 wt% of PVDF binder). Thus, 1:2 was used as the carbon to sulfur ratio in the further optimization experiments.

Table 1
Summary of the capacities derived from each step of cell reactions in Li–S batteries.

C/S ratio	Capacity delivered at the plateau of 2.3 V (mA h g^{-1}-sulfur)	Capacity delivered at the plateau of 2.1 V (mA h g^{-1}-sulfur)	Capacity resulted from the reduction of $LiNO_3$ (mA h)[a]
1:3	262	174	0.07
1:2	312	538	0.09
1:1	328	758	0.12
2:1	303	660	0.28
3:1	300	656	0.30
Theoretical value	418	1254	0.78

[a] The capacity is calculated based on the reaction: $LiNO_3 + 2Li^+ + 2e \rightarrow LiNO_2 + Li_2O$.

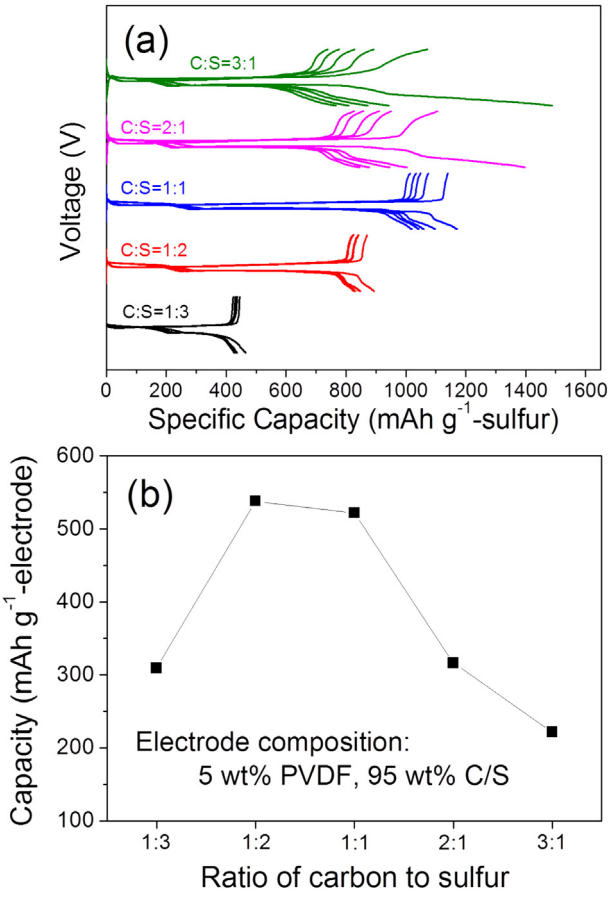

Fig. 1. Li–S battery performance of C/S composites with varied ratio of carbon black to sulfur: (a) voltage profiles in the first 5 cycles and (b) the relationship between electrode capacity (2nd cycle) and C/S ratio. The loading density of C/S composite was 1.7 mg cm^{-2} and the volume of electrolyte used was 20 μL. The applied current density is 56.6 μA cm^{-2}.

3.2. *Effects of sulfur loading and electrolyte volume on the electrode specific capacity*

Active material loading in electrode significantly impacts the energy density of an electrode. In a commercial Li-ion battery, the

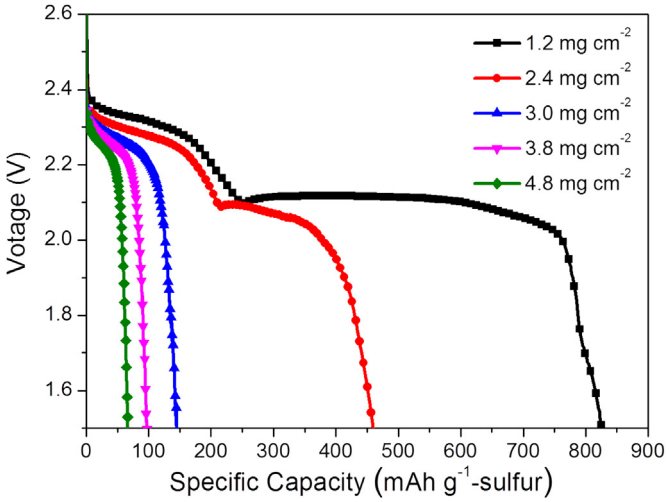

Fig. 2. Initial discharge voltage profiles of the C/S composite (C:S = 1:2) with different sulfur loading density (mg cm^{-2}) and the volume of electrolyte used was 20 μL. The applied current density is 56.6 μA cm^{-2}.

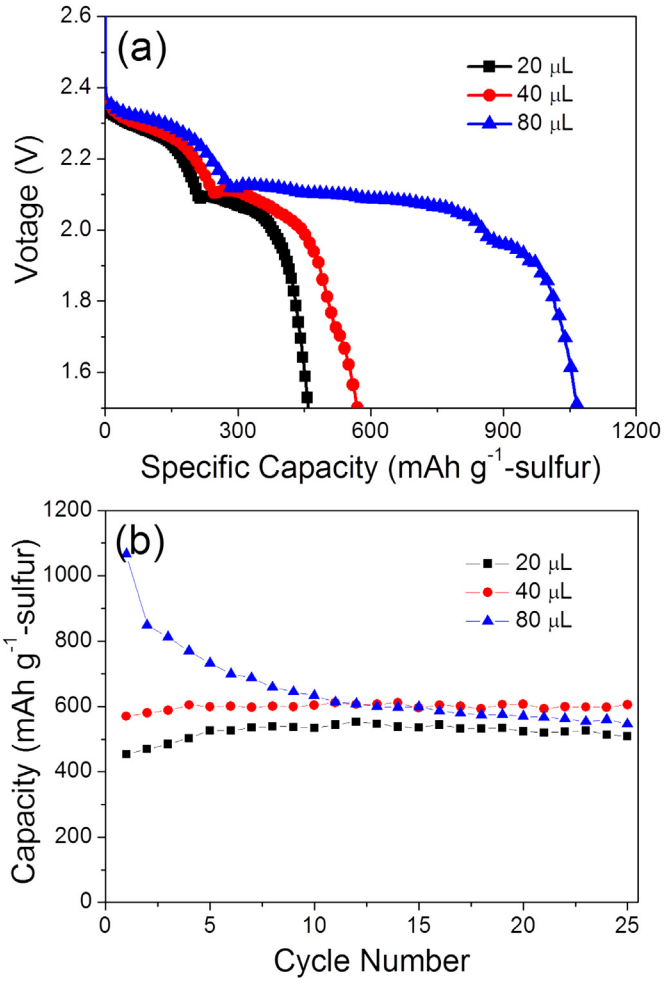

Fig. 3. Electrochemical performance of the C/S composite (C:*S* = 1:2) cycled in different volume of electrolyte: (a) initial discharge voltage profiles and (b) cycling performance. The sulfur loading density was 2.4 mg cm^{-2} and The applied current density is 56.6 μA cm^{-2}.

energy density of $LiCoO_2$ electrode is generally about 2.7 mA h cm^{-2} which is higher than that of S/C electrode with a typical value of 1.1 mA h cm^{-2}. To improve the energy density of S/C electrode, one can increase loading of sulfur and/or thickness of electrode. In this work, thicker cathode films were prepared from slurry consisting of C/S composite (with C/S ratio of 1:2) and PVDF binder onto aluminum foils using doctor-blade casting. The discharge curves for S/C composite cathodes of different sulfur loading are displayed in Fig. 2. One can see that as the sulfur loading was increased from 1.2 to 2.4 mg cm^{-2}, the capacity per unit mass of sulfur was reduced by 45%–459 mA h g^{-1}-sulfur. This is likely caused by the incomplete conversion of Li_2S_n to Li_2S, as concluded from a shorter voltage plateau at 2.1 V. Further increase of sulfur loading, e.g. to 3.0 mg cm^{-2}, led to a sharp capacity fade where the disappearance of the voltage plateau at 2.1 V suggested Li_2S_n ($n = 6$, 8) as the final product of sulfur reduction in the discharge process. The partial reduction of sulfur may be attributed to the saturation of Li_2S_8/Li_2S_6 in the electrolyte, where these insoluble solids covered the unreacted sulfur and stopped further cell reaction. In this context, the volume of electrolyte also plays an important role in the capacity of the cell.

Generally, larger volume of electrolyte helps dissolve more PS during discharge and also better wet the electrode; however, the brought-in drawback is the decrease of the energy density. The effect of the electrolyte volume on the initial discharge voltage profiles of S/C composite cathodes was investigated, and the results are shown in Fig. 3a. It can be seen that as the electrolyte volume was increased from 20 to 40 μL, the capacity increases by 71 mA h g^{-1}-sulfur (cf. total changes from the voltage plateaus at 2.3 and 2.1 V). Such synchronous increase of cell capacities at two plateaus seems to indicate improved wetting of the electrode. As the electrolyte volume was further increased to 80 μL, the increase of capacity at 2.3 V was significantly slowed down (288 mA h g^{-1}-sulfur). Interestingly, more Li_2S_n were converted into Li_2S_2/Li_2S at the end of discharge which delivered a doubled capacity as 575 mA h g^{-1}-sulfur at 2.1 V. Furthermore, a clear voltage slope was observed which can be attributed to the reduction of $LiNO_3$. With sulfur loading of 2.4 mg cm^{-2} and electrolyte volume of 80 μL, a capacity of 1066 mA h g^{-1}-sulfur was delivered by the electrode. The initial capacity per square centimeter in this case can be as high as 2.8 mA h cm^{-2}. Nevertheless, increasing electrolyte volume is by no means a good way for the improvement of Li–S battery performance. Not only will the energy density drop at cell level, but also poor cell cyclic stability is rendered. This can be clearly seen from the testing results of a number of cells with different electrolyte volume, ranging from 20 to 80 μL, as shown in Fig. 3b. For Li–S cells with 20 and 40 μL of electrolyte, almost constant capacities of 550 and 600 mA h g^{-1}-sulfur are seen in the first 25 cycles. As a clear contrast, the cell with 80 μL of electrolyte showed a large initial capacity loss (119 mA h g^{-1}-sulfur). This could be due to the leftover of Li_2S_6 and Li_2S_4 in the electrolyte at the end of discharge [51]. Larger volume of electrolyte may work as a PS reservoir in the cell and also accelerates the PS transport from

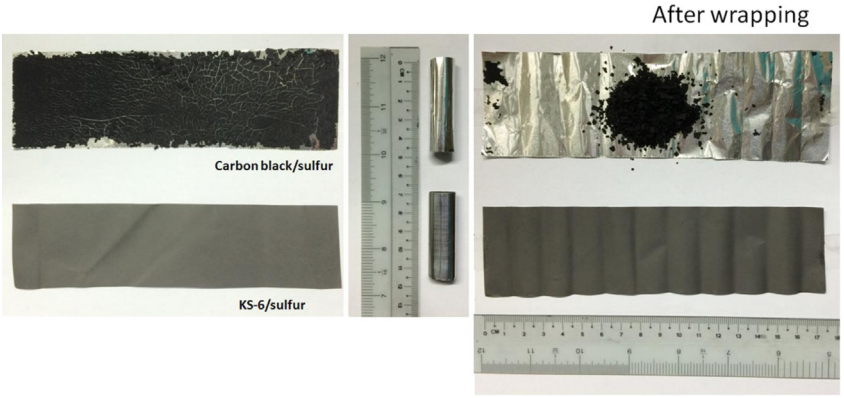

Fig. 4. Deformability test of electrodes (C:*S* = 1:2) prepared with carbon black and KS-6, with a sulfur loading density of 10 mg cm^{-2}.

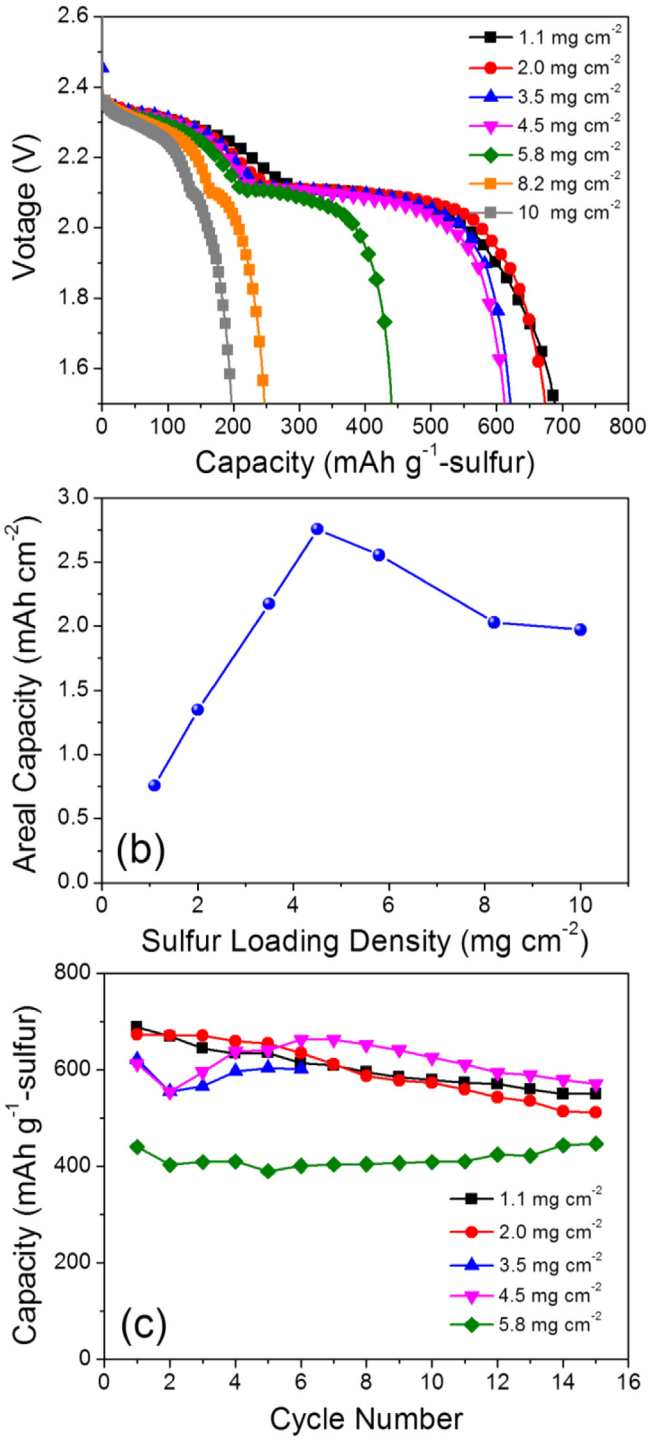

Fig. 5. (a) Initial discharge voltage profiles, (b) the curve of areal capacity vs. sulfur loading density and (c) cycling performance of the KS-6/sulfur composite (C:*S* = 1:2) with different sulfur loading density (mg cm^{-2}). The volume of electrolyte used was 80 μL and the applied current density is 56.6 μA cm^{-2}.

cathode to Li anode, giving rise to a fast capacity fading. Such fast capacity drop in the first a few cycles is often seen in the study of Li–S batteries [13,31,40,41] which however can be suppressed if the carbon microstructure is modified to be better PS absorbent [25]. The optimization of the ratio between sulfur and liquid electrolyte has been systematically investigated and reported recently by Zheng et al. [52].

3.3. Improvement of bonding performance

The fast capacity fading of the cell with large volume of electrolyte suggests the need of even higher sulfur loading density on cathode current collector to improve the energy density; however, thicker films from composite of sulfur and carbon black of high surface area are brittle and tend to peel off from the current collector, as shown in Fig. 4. This situation is significantly improved by replacing carbon black with conductive fine graphite powders (KS-6). With KS-6 the sulfur loading density can be as high as 10 mg cm^{-2} and the electrode film shows good mechanical properties for wrapping and pressing.

The initial discharge voltage profiles of KS-6/sulfur composite (C:*S* = 1:2) with varied sulfur loading density are shown in Fig. 5a. A volume of 80 μL of electrolyte was universally used to ensure completely wetted electrodes. At sulfur loading density of below 4.5 mg cm^{-2}, a similar capacity in the range of 612–688 mA h g^{-1}-sulfur was delivered. As sulfur loading density was increased to 5.8 mg cm^{-2}, the capacity dropped to 440 mA h g^{-1}-sulfur. With further increasing the sulfur loading density to 10 mg cm^{-2}, the cell can only retain a capacity of 197 mA h g^{-1}-sulfur. The corresponding areal capacities at varied sulfur loading density are calculated to be 0.76 (1.1 mg cm^{-2}), 1.35 (2.0 mg cm^{-2}), 2.17 (3.5 mg cm^{-2}), 2.77 (4.5 mg cm^{-2}), 2.55 mA h cm^{-2} (5.8 mg cm^{-2}), 2.03 mA h cm^{-2} (8.2 mg cm^{-2}) and 1.97 mA h cm^{-2} (10.0 mg cm^{-2}) respectively (Fig. 5b). With sulfur loading density of 4.5 mg cm^{-2} the power density of the electrode reached 5.88 mW h cm^{-2}. Using the KS-6/S composites on electrodes leads to 58–63% of capacity loss in comparison to their counterparts using carbon black/S composites; however, good cyclic performance is observed (Fig. 5c). Lower capacities of KS-6/sulfur composites are also seen in the shortened voltage plateau at 2.1 V, which is likely attributed to the lower surface area of KS-6 (affects the extent of Li_2S_4 to Li_2S_2/Li_2S conversion). Introduction of additional carbon materials with large surface area that helps provide more precipitation sites for Li_2S_n, e.g. activated carbon, may be the solution to compensate the capacity loss caused by the use of KS-6/sulfur composite.

4. Conclusions

The performance of a Li–S battery is affected by multiple parameters. Electrolyte volume, carbon/sulfur ratio and sulfur loading density, as well as the choice of carbon source impact the battery performance in terms of capacity, cycleability, and processibilities. The C/S composite may deliver a capacity of 538 mA h g^{-1}-electrode which is 3 times as high as that of $LiCoO_2$. The capacity per square centimeter can be improved with higher sulfur loading density. Sulfur loading density can be further increased by replacing carbon black with fine graphite powders. With these optimizations the electrode delivers a power density of 5.88 mW h cm^{-2} which is 60% of the commercial $LiCoO_2$ electrode.

Acknowledgments

This research was supported by the Advanced Energy Storage Research Programme (IMRE/12-2P0503 and IMRE/12-2P0504), Institute of Materials Research and Engineering (IMRE) of the Agency for Science, Technology and Research (A*STAR), Singapore.

References

[1] J.M. Tarascon, M. Armand, Nature 414 (2001) 359–367.
[2] J.B. Goodenough, Y. Kim, Chem. Mater. 22 (2010) 587–603.
[3] F. Leroux, G. Goward, W.P. Power, L.F. Nazar, J. Electrochem. Soc. 144 (1997) 3886–3895.
[4] J. Liu, H. Xia, D. Xue, L. Lu, J. Am. Chem. Soc. 131 (2009) 12086–12087.

[5] Y. Wang, G.Z. Cao, Chem. Mater. 18 (2006) 2787–2804.
[6] X. Feng, N. Ding, Y. Dong, C. Chen, Z. Liu, J. Mater. Chem. A 1 (2013) 15310–15315.
[7] A. Debart, J. Bao, G. Armstrong, P.G. Bruce, J. Power Sources 174 (2007) 1177–1182.
[8] X. Ji, L.F. Nazar, J. Mater. Chem. 20 (2010) 9821–9826.
[9] C.P. Yang, S. Xin, Y.X. Yin, H. Ye, J. Zhang, Y.G. Guo, Angew. Chem. Int. Ed. 52 (2013) 8363–8367.
[10] S.S. Zhang, J. Power Sources 231 (2013) 153–162.
[11] P.G. Bruce, S.A. Freunberger, L.J. Hardwick, J.M. Tarascon, Nat. Mater. 11 (2012) 19–29.
[12] W.J. Chung, J.J. Griebel, E.T. Kim, H. Yoon, A.G. Simmonds, H.J. Ji, P.T. Dirlam, R.S. Glass, J.J. Wie, N.A. Nguyen, B.W. Guralnick, J. Park, A. Somogyi, P. Theato, M.E. Mackay, Y.E. Sung, K. Char, J. Pyun, Nat. Chem. 5 (2013) 518–524.
[13] Z.W. Seh, W. Li, J.J. Cha, G. Zheng, Y. Yang, M.T. McDowell, P.C. Hsu, Y. Cui, Nat. Commun. 4 (2013) 1331.
[14] G. Zhou, S. Pei, L. Li, D.W. Wang, S. Wang, K. Huang, L.C. Yin, F. Li, H.M. Cheng, Adv. Mater. 26 (2014) 625–631.
[15] G. Zheng, Q. Zhang, J.J. Cha, Y. Yang, W. Li, Z.W. Seh, Y. Cui, Nano Lett. 13 (2013) 1265–1270.
[16] N. Jayaprakash, J. Shen, S.S. Moganty, A. Corona, L.A. Archer, Angew. Chem. Int. Ed. 50 (2011) 5904–5908.
[17] J. Zheng, J. Tian, D. Wu, M. Gu, W. Xu, C. Wang, F. Gao, M.H. Engelhard, J.-G. Zhang, J. Liu, J. Xiao, Nano Lett. 14 (2014) 2345–2352.
[18] S. Xin, L. Gu, N.H. Zhao, Y.X. Yin, L.J. Zhou, Y.G. Guo, L.J. Wan, J. Am. Chem. Soc. 134 (2012) 18510–18513.
[19] J.T. Lee, Y. Zhao, S. Thieme, H. Kim, M. Oschatz, L. Borchardt, A. Magasinski, W.I. Cho, S. Kaskel, G. Yushin, Adv. Mater. 25 (2013) 4573–4579.
[20] J. Schuster, G. He, B. Mandlmeier, T. Yim, K.T. Lee, T. Bein, L.F. Nazar, Angew. Chem. Int. Ed. 51 (2012) 3591–3595.
[21] L. Ji, M. Rao, H. Zheng, L. Zhang, Y. Li, W. Duan, J. Guo, E.J. Cairns, Y. Zhang, J. Am. Chem. Soc. 133 (2011) 18522–18525.
[22] G. He, S. Evers, X. Liang, M. Cuisinier, A. Garsuch, L.F. Nazar, ACS Nano 7 (2013) 10920–10930.
[23] W. Li, G. Zheng, Y. Yang, Z.W. Seh, N. Liu, Y. Cui, Proc. Natl. Acad. Sci. U. S. A. 110 (2013) 7148–7153.
[24] J. Gao, H.D. Abruna, J. Phys. Chem. Lett. 5 (2014) 882–885.
[25] X. Ji, K.T. Lee, L.F. Nazar, Nat. Mater. 8 (2009) 500–506.
[26] J. Jin, Z. Wen, G. Ma, Y. Lu, Y. Cui, M. Wu, X. Liang, X. Wu, RSC Adv. 3 (2013) 2558–2560.
[27] H. Wang, Y. Yang, Y. Liang, J.T. Robinson, Y. Li, A. Jackson, Y. Cui, H. Dai, Nano Lett. 11 (2011) 2644–2647.
[28] J. Guo, Y. Xu, C. Wang, Nano Lett. 11 (2011) 4288–4294.
[29] L. Yuan, H. Yuan, X. Qiu, L. Chen, W. Zhu, J. Power Sources 189 (2009) 1141–1146.
[30] M.Q. Zhao, X.F. Liu, Q. Zhang, G.L. Tian, J.Q. Huang, W. Zhu, F. Wei, ACS Nano 6 (2012) 10759–10769.
[31] W. Zhou, Y. Yu, H. Chen, F.J. DiSalvo, H.D. Abruna, J. Am. Chem. Soc. 135 (2013) 16736–16743.
[32] W. Weng, V.G. Pol, K. Amine, Adv. Mater. 25 (2013) 1608–1615.
[33] J.T. Lee, Y. Zhao, H. Kim, W.I. Cho, G. Yushin, J. Power Sources 248 (2014) 752–761.
[34] S. Moon, Y.H. Jung, W.K. Jung, D.S. Jung, J.W. Choi, D.K. Kim, Adv. Mater. 25 (2013) 6547–6553.
[35] Y. Yang, G. Yu, J.J. Cha, H. Wu, M. Vosgueritchian, Y. Yao, Z. Bao, Y. Cui, ACS Nano 5 (2011) 9187–9193.
[36] G. Zheng, Y. Yang, J.J. Cha, S.S. Hong, Y. Cui, Nano Lett. 11 (2011) 4462–4467.
[37] G. He, X. Ji, L. Nazar, Energy Environ. Sci. 4 (2011) 2878–2883.
[38] L.L. Peng, G.B. Liu, Y. Wang, Z.L. Xu, H. Liu, J. Solid State Electrochem. 18 (2014) 935–940.
[39] J. Song, T. Xu, M.L. Gordin, P. Zhu, D. Lv, Y.B. Jiang, Y. Chen, Y. Duan, D. Wang, Adv. Funct. Mater. 24 (2014) 1243–1250.
[40] T. Xu, J. Song, M.L. Gordin, H. Sohn, Z. Yu, S. Chen, D. Wang, ACS Appl. Mater. Interfaces 5 (2013) 11355–11362.
[41] L.X. Miao, W.K. Wang, A.B. Wang, K.G. Yuan, Y.S. Yang, J. Mater. Chem. A 1 (2013) 11659–11664.
[42] S.S. Zhang, Electrochem. Commun. 31 (2013) 10–12.
[43] J. Zheng, M. Gu, H. Chen, P. Meduri, M.H. Engelhard, J.-G. Zhang, J. Liu, J. Xiao, J. Mater. Chem. A 1 (2013) 8464–8470.
[44] S.S. Zhang, Energies 5 (2012) 5190–5197.
[45] Y.V. Mikhaylik, U.S. Patent (2008) 7,352,680.
[46] S. Urbonaite, P. Novak, J. Power Sources 249 (2014) 497–502.
[47] J. Zheng, M. Gu, C. Wang, P. Zuo, P.K. Koech, J.-G. Zhang, J. Liu, J. Xiao, J. Electrochem. Soc. 160 (2013) A1992–A1996.
[48] S.S. Zhang, Electrochim. Acta 70 (2012) 344–348.
[49] D. Aurbach, E. Pollak, R. Elazari, G. Salitra, C.S. Kelley, J. Affinito, J. Electrochem. Soc. 156 (2009) A694–A702.
[50] J. Zheng, M. Gu, M.J. Wagner, K.A. Hays, X. Li, P. Zuo, C. Wang, J.-G. Zhang, J. Liu, J. Xiao, J. Electrochem. Soc. 160 (2013) A1624–A1628.
[51] Y. Diao, K. Xie, S. Xiong, X. Hong, J. Electrochem. Soc. 159 (2012) A421–A425.
[52] J. Zheng, D. Lv, M. Gu, C. Wang, J.-G. Zhang, J. Liu, J. Xiao, J. Electrochem. Soc. 160 (2013) A2288–A2292.